

Concept Paper

# Developing Vulnerability Index to Quantify Urban Heat Islands Effects Coupled with Air Pollution: A Case Study of Camden, NJ

Samain Sabrin <sup>1,\*</sup> , Maryam Karimi <sup>2</sup> and Rouzbeh Nazari <sup>1</sup>

<sup>1</sup> Department of Civil, Construction, and Environmental Engineering, The University of Alabama at Birmingham, Hoehn Engineering Building, Birmingham, AL 35294, USA; rnazari@uab.edu

<sup>2</sup> Department of Environmental Health Science, The University of Alabama at Birmingham, School of Public Health, Ryals Public Health Building (RPHB), Birmingham, AL 35294, USA; karimi@uab.edu

\* Correspondence: sabrins8@uab.edu

Received: 12 April 2020; Accepted: 25 May 2020; Published: 27 May 2020



**Abstract:** Extreme heat events at urban centers in combination with air pollution pose a serious risk to human health. Among these are financially distressed cities and neighborhoods that are facing enormous challenges without the scientific and technical capacity for planning and mitigation. The city of Camden is one of those economically distressed areas with a predominantly minority population, a high unemployment rate, high poverty rates, and poor air quality (PM<sub>2.5</sub> and ozone), and it remains vulnerable to heat events. This paper focuses on studying a coupled effect of Urban Heat Islands (UHIs) and Ozone-PM<sub>2.5</sub> pollution at the neighborhood-scale in the city of Camden, using fine scale remotely sensed land-surface temperature and air quality data from the Community Multiscale Air Quality (CMAQ) Modelling System in the Geographic Information Systems (GIS) platform. To assess the impact of urban microclimate on the city of Camden, NJ, residents' health, we identified several environmental and social parameters as the root causes of vulnerability imposed by extreme-heat and poor air quality. Vulnerability in terms of environment and social wellbeing was spatially quantified as two conceptual vulnerability-index models (i.e., environmental vulnerability index (EVI) and a social vulnerability index (SVI)) using multiple linear regression algorithm. Factors such as remotely sensed earth surface properties, built-environment components, air quality, and socio-economic data were incorporated in a holistic geographic approach to quantify the combined effect. Surface temperature gradient and Proportional Vegetation ( $P_v$ ) generated from 30 m resolution Landsat 8 were sampled along with other variables in the city of Camden, NJ. Models incorporating  $P_v$  suggest better fit than models with normalized difference vegetation index (NDVI). Water fraction (33.5%, 32.4%), percentage imperviousness (32.5%, 32%),  $P_v$  (20.5%, 19.6%), and digital elevation model (DEM) (9%, 8%) have the highest contributions in both models. Two output maps identified the vulnerable neighborhoods in the city through comprehensive GIS analysis: Lanning Square, Bergen Square, Central Waterfront, Gateway, Liberty Park, and Parkside. This can provide useful information for planners and health officials in targeting areas for future interventions and mitigations.

**Keywords:** air quality; CMAQ; environmental risk; impact index; social risk; UHI

## 1. Introduction

Pervious lands converted to impermeable surfaces in the process of global urban sprawl has induced serious environmental issues in major metropolitan cities [1], leading to an increased heat effect in urban canopies [2]. Urban Heat Islands (UHIs) effects are generally observed in cities

with dense building structures and areas mostly covered with heat absorbing pave materials, which sustain prolonged periods of high surface and air temperature. UHIs have been spatially linked with the regional land-use changes [3] and are intensified due to the trapped heat by greenhouse gas emission [4]. Studies show cities larger than 500 km<sup>2</sup> experienced a rise of 4.7 °C in average daytime summer temperature over three annual cycles of 2003–2005 [5]. Air temperatures have been elevating by 0.24 °C and 0.16 °C per decade in cities and rural areas of the U.S., respectively [6]. With increasing heat and humidity in the summers, mortality rate has increased significantly in northern U.S. cities [7–9]. Considering the Bjerknes Centre for Climate Research Bergen Climate Model, version 2.0 (BCCR-BCM2.0) climate scenario, the additional global heat-related mortalities will be 92,207 in 2030 and 255,486 in 2050 if we do not take appropriate actions to mitigate the adverse effects of actual or expected future climate [10]. The elevated temperature patterns along with air pollution not only cause thermal and physical discomfort, but also create major health hazards for the vulnerable population living in cities. The concentrations of fine particulate matter (smaller than 2.5 µm in aerodynamic diameter-PM<sub>2.5</sub>) and ozone in ambient air have been linked to the incidence of premature mortality and morbidity outcomes in recent studies along with the adverse health impacts by other anthropogenic air pollutants [11–14]. Moreover, some researchers have associated the increasing trend of temperatures with air pollution [15,16]. Hence, planners, policymakers, and public health professionals are now focusing on the mitigation strategies, which require an integrated approach covering the multi-sectors of a society. The impact of mitigation techniques has shown to reduce heat-stress and can also benefit social wellbeing [17]. Prior to implementing such strategies, it is essential to have a broad picture of the societal and environmental vulnerabilities to be prioritized for the interventions. This study can be an intermediate platform to navigate through the social and environmental aspects prone to vulnerability due to both UHIs effect and poor air quality.

Over the last two decades, the growth of urban areas and increased concentrations of city-dwellers have directed more attention to this topic. The vulnerability to any extreme weather event greatly depends on the adaptive capacity and the socio-economic factors of a community. Vulnerability can be defined by the social, physical, environmental, and economic processes and institutional structures that determine a system's adaptation capacities in responding to dangers [18]. Exposure, sensitivity, and adaptive capacity are the three components of vulnerability and represent the share of the exposed population, the degree to which people react to a threat, and the ability (financial resources, health) to overcome negative impacts, respectively [19–22]. A better understanding of the UHI phenomena within a city's context is important to make a city more resilient to UHIs effects [21]. Risk factors in the neighborhood level can contribute to climate vulnerability in cities [23]. For example, socio-economic parameters of a community such as economic status, wellbeing, population density, individual's age (infants and elderly population over 65 years), education level, employment, people living alone, and health security may influence social vulnerability to air pollution and heat events [24–27]. Also, higher heat-related mortality was observed in neighborhoods with very little to no tree canopy, which are more evident in lower income communities and elderly populations [7,28,29]. With some regions suffering more than others, climate modelling results from 2007–2069 predict higher numbers of heat-related mortality in the 65+ age-group communities in the Northeastern states [7].

Previously, a heat vulnerability index (HVI) was developed for Greater London in the United Kingdom to manage heat-related health issues [30]. Vulnerability to high temperature was mapped for the city of San Juan (capital of Puerto Rico) via a heat vulnerability index (HVI), which was developed using satellite images combined with the census data [31]. A framework was proposed integrating social and health sciences approaches to understand indoor and outdoor exposure risk by air pollution and extreme heat [32]. Moreover, several mitigative and adaptive strategies in response to UHIs have been assessed for the cities of Westminster, Maryland [33], and Vancouver, BC [34], and the cooling benefits of green roofs as a mitigative response were evaluated for the city of Detroit, Michigan [35]. A recent paper reviewed the impact of present and future UHIs in the context of energy, peak electricity demand, air quality, mortality and morbidity, and urban vulnerability [36]. Although the UHIs

phenomena have been extensively studied in more than 400 cities around the world, their impacts on air quality and consequently human health have not been sufficiently evaluated or quantified to educate the public. In order to implement proper interventions, health officials and planners need fine scale information that identifies the risk of exposure at the neighborhood level.

This paper focuses on studying a coupled effect of UHIs and Ozone-PM<sub>2.5</sub> pollution at the neighborhood-scale in the city of Camden, New Jersey, using fine scale remotely sensed land-surface temperature and air quality data from the Community Multiscale Air Quality (CMAQ) Modelling System in the Geographic Information Systems (GIS) platform. Solecki et al. [37] studied UHIs events in the region of greater Camden and proposed mitigation strategies for the neighboring communities. The impacts of UHIs on the community's social and environmental vulnerability was not further investigated in the study. In 2005, the benefits of urban vegetation and using reflective roofs as mitigation strategies were proposed for the city [38]. However, despite many recent changes in the city's urban environment, there have been no in-depth studies of Camden that tie UHIs to community health and the environment for the last 15 years. The objective of this study is to create high-resolution index maps to identify communities and areas in need of neighborhood-specific risk mitigation and response strategies. The main value of the high-resolution temperature model is realized by: (a) identifying neighborhoods that tend to heat up and experience poor quality air, (b) determining the most vulnerable population within the study area, and (c) determining how changes in the land-cover conditions could alter the ambient temperature gradients over the long term. As a final output, we generated an index system with an intent to help planners and public-health professionals in identifying highly exposed neighborhoods to the extreme heat and air pollution zones. Our proposed index can be a useful tool to assist decision making in the case of emergency and it can provide guidance for city-planners and emergency medical services.

## 2. Study Area

Camden is the fifth largest city in New Jersey, with a population number of 76,005 and 10.36 square miles land area. An economically distressed area of the state, the city has a major issue of high unemployment and 40% poverty rates [39]. One-third of its land cover is used for manufacturing and industrial activities, more than half of which are marked as brownfield areas. Besides environmental contamination from the abandoned industries, there is significant air, soil, and water pollution in the city of Camden [40]. UHIs in the city were clearly identified in both the climate data and satellite images [37]. The overall climate of the greater Camden region has been warming by approximately 0.2 °C per decade during the year span of 1955–1999, while the highly urbanized city areas within the region have been warming at the even rapider rate of 0.33 °C per decade [37]. Camden was ranked second among the ten most densely populated U.S. cities with more than 100 days of elevated PM<sub>2.5</sub> and ozone concentration [41]. New Jersey State Health Assessment Data also ranked Camden as the top third city (2011–2014) for asthma hospitalizations [42], which retained the same position in 2016 (shown in Figure 1). The figure also addresses the severity of social vulnerability in terms of poverty rate, where 9 of 19 census tracts in the city have a population range of 3791–6617 living under extreme poverty in each tract. Recently, the 20th annual "State of the Air" report by the American Lung Association graded the city with an "F" for air quality. Therefore, a densely populated city with a high poverty rate such as Camden possesses higher risk for the inhabitants in tackling the health impact related to heating events and air pollution.

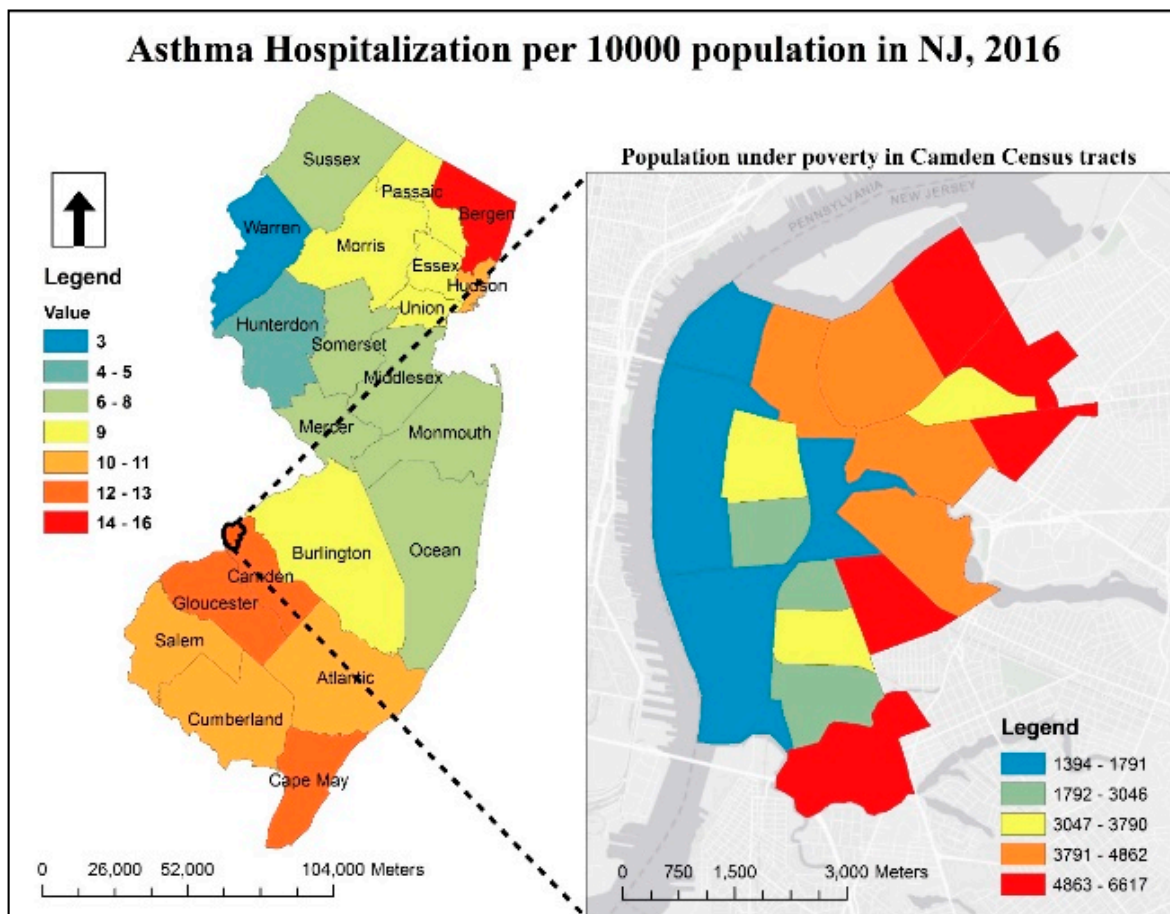


**Figure 1.** Asthma hospitalization crude rate per 10,000 population in New Jersey counties and population under poverty in Camden census-tracts in 2016.

### 3. Methodology

Prior to developing our conceptual models, we studied several parameters that have a possible correlation with the extreme heating events and air pollution in urban settings, which have been identified and discussed in previous literature [2,24–27,43,44]. Vulnerability to heat-stress can vary depending on the types of infrastructure, culture, climate, and many other factors [45]. Populations aged below 5 and above 65 struggle to cope with extreme environment and pollution. Both air temperature and land surface temperature (LST) can be affected by large portions of tall and wide buildings, as well as their footprints, by releasing absorbed heat to the environment. Likewise, UHIs are intensified by the higher density of buildings and population, while greeneries and vegetation cool surrounding environments through evapotranspiration and by providing shade. Studies have observed an association between the harmful effect of elevated temperature and poor air quality on mortality [46,47].

We developed two indices (i.e., the environmental risk impact index (ERII), and social vulnerability index (SVI)) in a holistic approach to quantify responsible parameters affecting air quality and UHIs for the city of Camden, NJ. The ERII index helps to identify locations associated with the greater environmental risk linked with UHI–air pollution and to suggest potential locations appropriate for environmental interventions. The SVI index can be used to identify areas in need of improved social parameters and wellbeing. We applied multiple linear regression algorithm model using ordinary least squares (OLS) on the spatially sampled data to quantify ERII and SVI index. The geo-referenced index points are summarized over the domain of census grids before mapping in GIS to identify the vulnerable neighborhoods. Figure 2 shows the step-by-step procedure used to calculate the environmental risk

and social vulnerability. Similarly, the most likely temperature patterns were identified based on the air pollution, amount of vegetation, building heights, and land coverage in the urban environments of Camden. The unique feature of this mapping tool is its integration of air quality and social data with climate/land data for predicting community risk and health hazards.

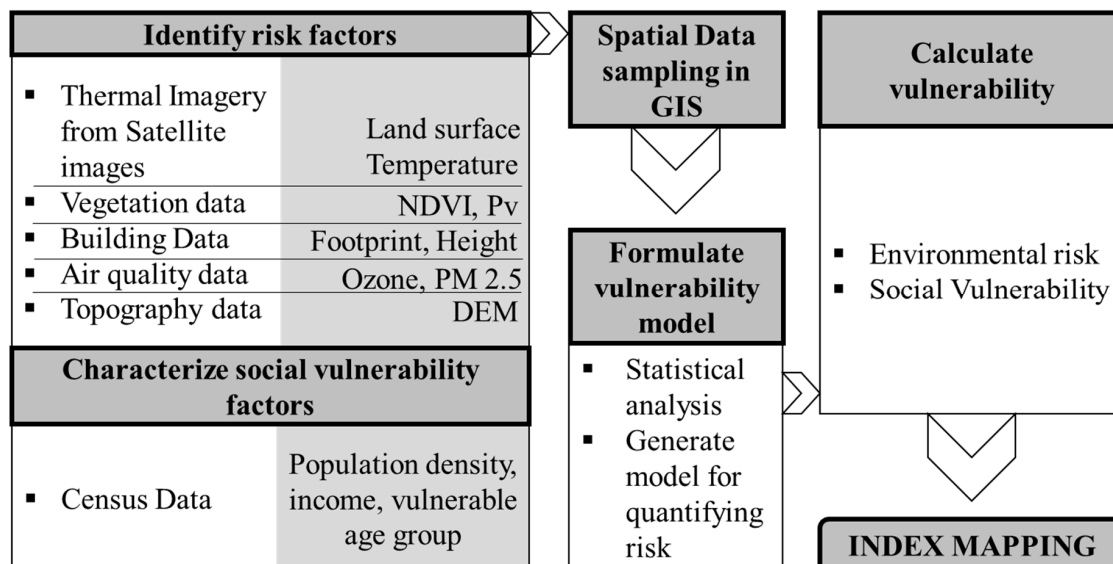


Figure 2. Step-by-step procedure to quantify vulnerability.

#### 4. Data Collection

Data for the environmental and socio-economic variables (mentioned in Figure 2 and listed in Table 1) were first collected within the study area to create vulnerability maps. The city has a deficiency in the canopy-scale temperature, air quality data, and consistent weather stations, which restricted us to study the spatial pattern of temperature and air pollution in high resolution. Camden has few weather stations within the city, and they are insufficient at providing more realistic and reliable data. The city mostly relies on a Philadelphia weather station located outside the city for weather forecast. Hence, temperature data were collected at fine spatial scales via the earth observation satellite Landsat 8 that incorporates the role of the built environment. Many studies [31,48–55] have used satellite data to derive surface temperature in high spatial resolution using the remote-sensing techniques in order to study UHIs effect over a large area. Therefore, we used Landsat 8 multispectral satellite images to obtain high resolution land surface temperature (LST) data and proportional vegetation ( $P_v$ ) using the equations described [56,57]. Landsat 8 images for 19 May 2014 were used to derive LST and  $P_v$  raster layers. The LST map seems to show larger regions with higher temperatures ranging between 32 °C and 43 °C, and  $P_v$  ranges from  $9.87 \times 10^{-17}$  to 2.97 (Figure 3).

Table 1. Environmental Risk Impact Index (ERII) and Social Vulnerability Impact Index (SVII) model parameters and summary results.

ERII Parameters (E)	Coefficient	VIF Value	Social Parameters (S)	Coefficient	VIF Value	Correlation with LST
Proportional vegetation ( $P_v$ )	-2.83 *** (b)	1.65	Proportional vegetation ( $P_v$ )	-2.683 *** (b')	1.71	0.65 ***
Water fraction ( $W_f$ )	-4.16 *** (c)	2.24	Water fraction ( $W_f$ )	-4.11 *** (c')	2.36	0.78 ***
Building footprint area ( $B_f^2$ )	0.35 *** (d)	1.23	Building footprint area ( $B_f^2$ )	0.37 *** (d')	1.24	0.17 ***
Building height ( $B_h^2$ )	0.025 ~ (e)	1.28	Building height ( $B_h^2$ )	0.007 ~ (e')	1.3	0.23 ***
DEM ( $E_m$ )	0.12 *** (f)	1.57	DEM ( $E_m$ )	0.094 *** (f')	1.8	0.46 ***
PM <sub>2.5</sub> concentration ( $P_m$ )	8.11 *** (g)	4.59	PM <sub>2.5</sub> concentration ( $P_m$ )	9.96 *** (g')	5.0	0.07 ***
Ozone concentration ( $O_2$ )	-3.26 *** (h)	4.36	Ozone concentration ( $O_2$ )	-4.26 *** (h')	4.72	0.05 ***
		2.04	% Imperviousness ( $I_m^2$ )	1.51 *** (i')	2.10	0.77 ***
% Imperviousness ( $I_m^2$ )	1.49 *** (i)		Population in <5 and >65 age group ( $P_a^2$ )	-0.09 *** (j)	2.04	0.06 ***
			Population density ( $P_d^2$ )	0.24 *** (k)	1.53	0.3 ***
			Monthly income ( $M_i^2$ )	0.06 *** (l)	1.94	0.1 ***

Table 1. Cont.

ERII Parameters (E)	Coefficient	VIF Value	Social Parameters (S)	Coefficient	VIF Value	Correlation with LST
Intercept (a)	118.84		Intercept (a')	152.9		
Adjusted R-squared	0.7734		Adjusted R-squared	0.7758		
Residual standard error	1.984		Residual standard error	1.973		

Note: Significance value  $\cdot = p < 0.5$ ,  $\cdot\cdot = p < 0.1$ ,  $\cdot\cdot\cdot = p < 0.05$ ,  $\cdot\cdot\cdot\cdot = p < 0.01$ , and  $\cdot\cdot\cdot\cdot\cdot = p < 0.001$ .

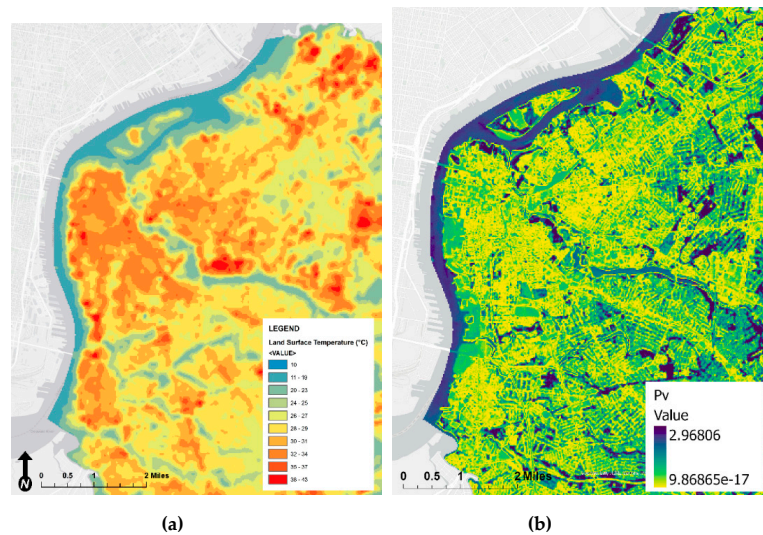


Figure 3. Environmental parameters mapped over Camden city: (a) land surface temperature (LST) in °C; (b) Proportional Vegetation ( $P_v$ ).

The urban microclimate is influenced by water bodies, wetlands, and the perviousness of the land. Hence, we extracted the water fraction data from the 2014 revised version of the 30 m resolution land-cover data provided by the National Land Cover Database (NLCD) and used the percent impervious surface from NLCD as an input to model (Figure 4). Since UHIs are reported to be more likely to form when the land elevation decreases [58], we determined the correlation between UHIs, imperviousness, water fraction, and the Digital Elevation Model (DEM) data within the area of our interest. We used data from a three-dimensional 1-m topobathymetric elevation model (TBDEM) for the New Jersey/Delaware sub-region, including the Delaware Estuary and adjacent coastline developed by the USGS Coastal and Marine Geology Program.

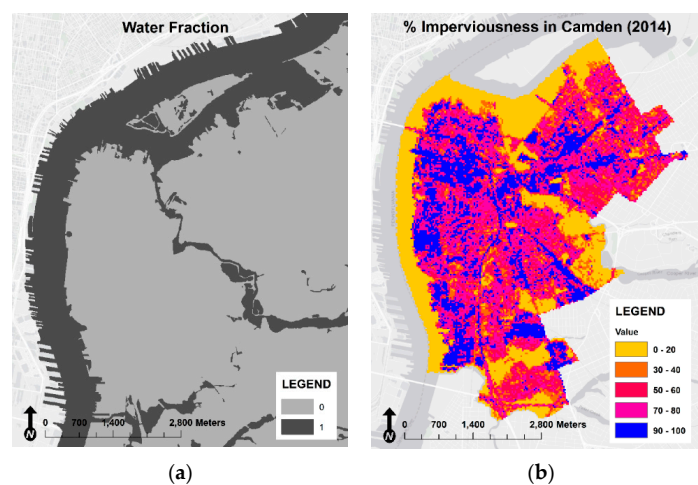
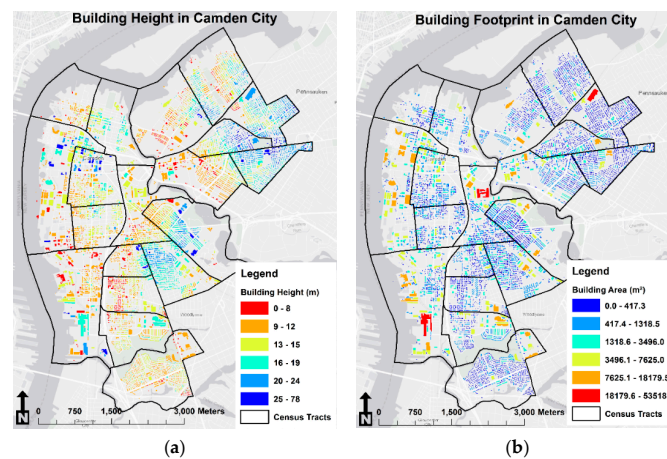


Figure 4. Environmental parameters mapped over Camden city: (a) water fraction (1 = water pixels, 0 = non-water pixels); (b) percent impervious area (%).

Much of the impervious fraction of land contains buildings, asphalt roads, and urban infrastructures that increase the amount of absorbed heat in urban settings. Large building footprints as well as tall and wide buildings can affect both LST and ambient air temperature. The UHIs impact is also governed by the height, area, and arrangement of these urban structures. To obtain the building areas and their locations in Camden, we collected geo-located building footprint data (first released by Microsoft in March 2017). Since no building height data are available for Camden, we downloaded LIDAR Point Cloud (LPC) data to extract building heights (Figure 5).



**Figure 5.** Environmental parameters mapped over Camden city: (a) building height (meters); (b) building area (meters<sup>2</sup>).

The city of Camden relies on just one air-quality station that is insufficient to study the spatial correlation between air quality and LST. Hence, we used the U.S. Environmental Protection Agency's (EPA) Fused Air Quality Surfaces Using Downscaling (FAQSD) tool and the Community Multiscale Air Quality (CMAQ) model as appropriate sources of air-quality data for our community level study (<https://www.epa.gov/hesc/rsig-related-downloadable-data-files>), which is downscaled to census-tracts level. We obtained ground level air quality data (ozone and PM<sub>2.5</sub>) for the same time period as LST. The CMAQ is an open-source development project by the U.S. EPA that provides (24-h) data on average PM<sub>2.5</sub> ( $\mu\text{g}/\text{m}^3$ ) and maximum 8-h average ozone (ppb). The red points in Figure 6 show the 24-h average PM<sub>2.5</sub> concentrations and maximum 8-h average ozone concentrations for May 19, 2014, at the centroid of each census tract.

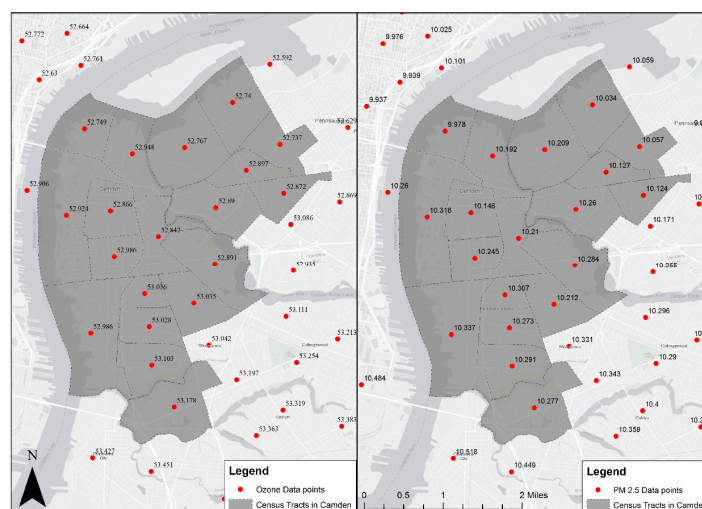


**Figure 6.** Community Multiscale Air Quality (CMAQ) data downscaled to centroid points of the census tracts: (left) ozone concentration in ppb; (right) PM<sub>2.5</sub> concentration in  $\mu\text{g}/\text{m}^3$ .

Since vulnerability to UHIs and poor air quality is a function of several social factors, we identified the vulnerable population by three major criteria: high population density, higher population in <5 and >65 age groups, and low monthly household income. Figure 7 maps the social parameters of our interest with data obtained from the 2010–2014 (five-year) estimates made by the American Community Survey. The census tracts colored in shades from orange to red in Figure 7 indicate the regions that meet these three susceptibility criteria.

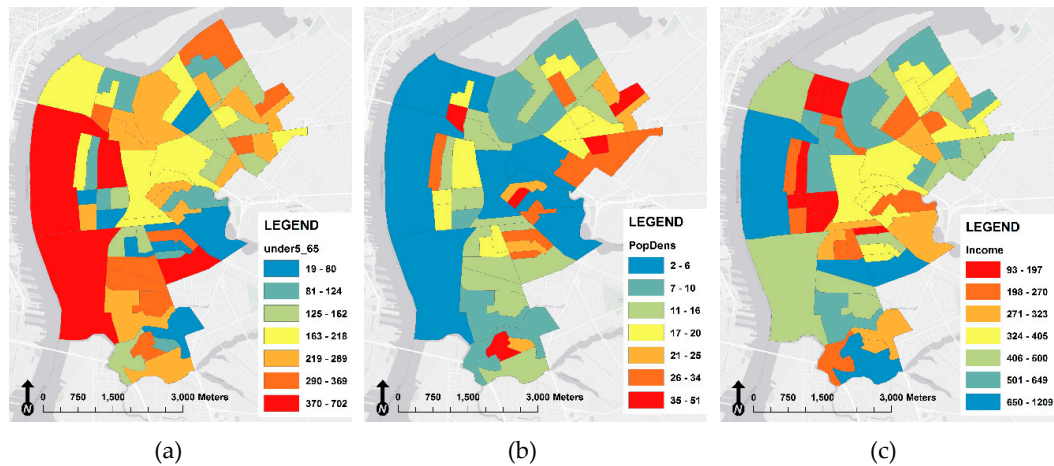


**Figure 7.** Social parameters mapped over Camden city: (a) population in age group of <5 and >65; (b) population density in block group; and (c) household income categorized within the census tracts of Camden.

## 5. Analysis and Discussion

### 5.1. Risk Index Models

All the environmental and socio-economic factors and health issues noted here seem to have an association with the UHIs effect and air pollution. The parameters listed in the previous section were first sampled at 20,000 points prior to examining the association among them in order to better understand their relationships. The correlation coefficient is referred to as statistically significant when this probability is less than 5% ( $p < 0.05$ ). Table 1 lists Pearson correlation coefficients at three levels of significance with  $p < 0.05$ ,  $p < 0.01$ , and  $p < 0.001$  for each value, which indicate only linear relationships between the variables. LST was found to be significantly correlated with % imperviousness (+0.77), proportional vegetation (−0.65), and water fraction (−0.78), and to be moderately linked with the DEM and weakly correlated with population density (+0.3). In the next step, to provide the best fit for the collected data set, regression analysis was performed with respect to the prediction potential of LST.

The risks for both environment and social vulnerability can be quantified using LST as the dependent variable in a multiple linear regression model, which can identify the significant explanatory parameters and their effects on LST. We developed two equally ranged indices as an estimation of vulnerability in terms of environmental and social impact. Our conceptual models calculate neighborhood risk in two different perspectives: Environmental Risk Impact Index (ERII) and Social Vulnerability Impact Index (SVII), using two separate formulas (1) and (2). Table 1 lists the independent variables of our interest in environmental and social categories and summarizes the results from the regression analysis.

$$\text{ERII} = f(E), \quad (1)$$

$$\text{SVII} = f(E, S). \quad (2)$$

### 5.2. Model Results

ERII was calculated as a function of environmental parameters, while SVII incorporates both environmental and social parameters. In order to detect any signs of multicollinearity within the models,

variation inflation factors (VIF) were tested to quantify the degree of inflations in the variances. The VIF values estimated for each parameter for ERII and SVII models have been listed in Table 1. In the ERII model, all parameters except PM<sub>2.5</sub> and ozone concentration have an inflation factor up to 2.04, implying low correlation with other predictors. The VIF values of PM<sub>2.5</sub> and ozone concentration are, respectively, 4.59 and 4.36 with moderate inflation. Similarly, parameters except for PM<sub>2.5</sub> and ozone in the SVI model are inflated by up to a factor of 2.36 with lower influence from the other regressors, while the air quality parameters show moderate inflation. The level of multicollinearity is moderate in the models. The plots of residual vs. fitted values show data points with no discernible pattern. Also, normal Q-Q plots for both models verify the assumption of normal distribution in the parameters. However, the models have been detailed in the Equations (3) and (4).

$$\text{ERII} = a + (b \cdot P_v + c \cdot W_f + d \cdot B_{fz} + e \cdot B_{hz} + f \cdot E_m + g \cdot P_m + h \cdot O_z + i \cdot I_{mz})_E, \quad (3)$$

$$\text{SVII} = a' + (b' \cdot P_v + c' \cdot W_f + d' \cdot B_{fz} + e' \cdot B_{hz} + f' \cdot E_m + g' \cdot P_m + h' \cdot O_z + i' \cdot I_{mz})_E + (j \cdot P_{az} + k \cdot P_{dz} + l \cdot M_{iz})_S. \quad (4)$$

However, where  $P_v$ ,  $W_f$ ,  $B_{fz}$ ,  $B_{hz}$ ,  $E_m$ ,  $P_m$ ,  $O_z$ ,  $I_{mz}$ ,  $P_{az}$ ,  $P_{dz}$ , and  $M_{iz}$  represent the proportional vegetation, water fraction, standardized building footprint area, standardized building height, digital elevation, PM<sub>2.5</sub> concentration, ozone concentration, standardized percent imperviousness, standardized population within <5 and >65 age-groups, standardized population density, and standardized average household monthly income (in dollars), respectively, the independent variables such as building area, height, % imperviousness, population aged <5 and >65, population density, and household monthly income have been standardized to improve the multicollinearity issue and maintain similar ranges in the coefficient values. The significance of all variables plugged in the models was proven with the adjusted R-squared values of 0.7734 and 0.7758, respectively ( $p < 0.05$ ), implying 77% of the fitted regression values were close to the observed data. The  $p$ -values of the individual variables are less than the significant level (0.05), and reject the null hypothesis of having no correlation with the dependent variable except for building-height in the ERII and SVII model. The buildings in the city were mostly observed to be low-rise buildings; hence, our sample for building height could not provide enough evidence of non-zero correlation with LST and did not contribute much to the models. Proportional vegetation, water-fraction, ozone concentration, and standardized population in vulnerable age groups having negative coefficients suggest that these variables increase with corresponding decrease in LST. The results show a higher positive coefficient for PM<sub>2.5</sub> concentration, indicating a possible increase in PM<sub>2.5</sub> with any increase in LST.

As a form of inferential statistics, the percent contributions of the independent attributes were calculated after performing regression analysis on the 11 independent variables. Relative weight analysis quantifies relative importance of the predictor variables in a regression analysis. The highest four contributors in both models were proportional vegetation, water fraction, percent imperviousness, and DEM of the land, with proportional vegetation being the highest. The ERII and SVII models were analyzed in two scenarios: one including proportional vegetation in the models and the other with NDVI. After conducting multiple linear regression analyses on both scenarios, the relative importance of the regressors was computed, as shown in Table 2. The contributions of NDVI for all three models were negligible compared to the contributions of  $P_v$ . Therefore, our final regression models were designed considering  $P_v$  as an important contributor.

This paper has identified the most likely patterns in temperature in relation to air pollution, amount of vegetation, building height, and land coverage in an urban environment for the city of Camden. The ERII and SVI index maps have been generated for a single day (19 May 2014) as an example, and can be replicated for the whole summer to conduct an annual risk assessment. The time-dependent effects on both indices will be dominated by LST,  $P_v$ , and air pollution data, as these parameters will change on daily basis.

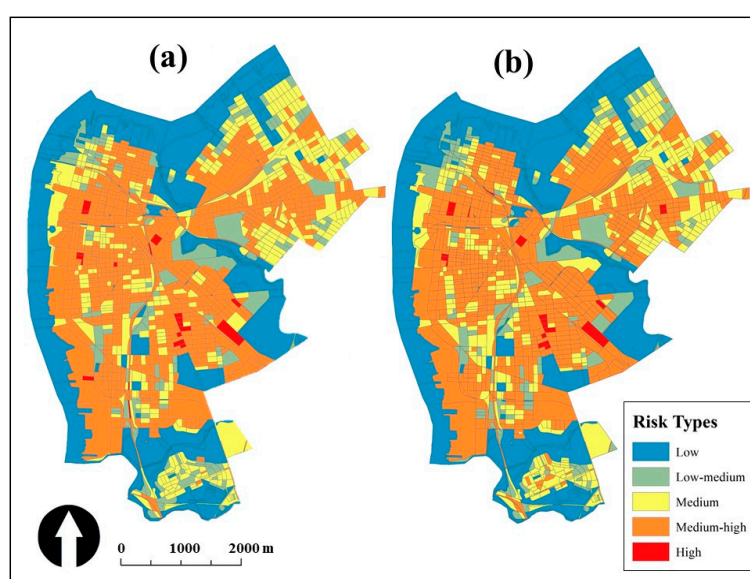
**Table 2.** ERII and SVII model parameters and summary results.

Variables	Relative Weights of Variables (%)	
	ERII	SVII
Proportional Vegetation	20.5	19.6
Water Fraction	33.5	32.4
Building footprint Area	1.6	1.7
Building height	1.6	1.5
DEM	9.0	8.0
PM <sub>2.5</sub>	0.9	1.2
Ozone	0.4	0.5
% Imperviousness	32.5	32.0
Population Density	-	2.9
Monthly Income	-	0.3
Population <5 & >65	-	0.2

### 5.3. Index Mapping to Identify Vulnerability

The ERII, and SVII indices were normalized using the method of minimum-maximum normalization to maintain the similar range [59]. Both indices have been categorized in 5 risk types depending on their ranges. The risk associated with any census grid is designated as low, low-medium, medium, medium-high, and high when its index falls within the range of '0–5.5', '5.5–6', '6–6.5', '6.5–7.3', and '7.3–10', respectively. Nearly 53–56% of census grids lie within the domains of medium-high and high ERII and SVI indices.

We observed in our study that an index of 7.3 associates with  $>32$  °C in both indices, which can lead to detrimental health effects such as heat cramps and exhaustion. Therefore, we categorized ERII and SVII index higher than 7.3 as high-risk indicating extreme exposure to UHIs and air pollution. ERII and SVII for all census grids in Camden have been mapped using ArcGIS software. Figure 8 illustrates two index maps identifying the neighborhoods of Lanning Square, Bergen Square, Central Waterfront, Gateway, Liberty Park, and Parkside as areas most environmentally and socio-economically vulnerable to UHIs. The risk types for the grids are colored in the scheme from dark red to blue, denoting red colored grids as the highly vulnerable area. The spatially mapped index can indicate the potential locations to prioritize environment, economic, and health-service interventions.

**Figure 8.** ERII (a) and SVII (b).

## 6. Conclusions

UHIs phenomena observed in all growing cities directly affect local temperature and air quality and contribute to the long-term global distress in temperature and environment. As the global population moves more towards urban regions, we cannot deny the direct impact of the growing number of cities. This requires more interventions in the city planning to protect city-dwellers from consequential health issues. Heat exhaustion, heat stroke, and even deaths are triggered by extreme heat events, especially in the vulnerable populations. The index system discussed here will better communicate the risk for heat-related illnesses and death to the proper individuals, whether local officials to know to issue heat advisories, hospitals to allocate resources more efficiently, or private citizens so they are aware of the increased risk to themselves.

The result of this study concluded that proportional vegetation is a better explanatory variable than the Normalized Difference Vegetation Index (NDVI). The water fraction, % imperviousness, proportional vegetation of the land surface characteristics, and DEM were the highest contributors in our models. The *p*-values of the individual variables indicate correlation with LST except building-height in the ERII and SVII model. Nearly 53–56% of census grids lie within the domains of medium-high and high ERII and SVI indices. Moreover, Lanning Square, Bergen Square, Central Waterfront, Gateway, Liberty Park, and Parkside were identified as significantly exposed neighborhoods to heat and air pollution, while also being home to the most vulnerable populations. The methods applied in this study identify risk in two aspects: environmental and social wellbeing. Therefore, the ERII model can assist urban planners in careful planning or redesigning of the identified areas, while the SVII model will guide social workers and public health professionals towards proper community wellbeing intervention for the neighborhoods with high SVII values.

Annual risk assessment over subsequent years applying the proposed indices can contribute to guidance on where neighborhood heat awareness programs are most needed and also can provide enhanced neighborhood-specific guidance on green infrastructure developments and the improved decision-making capacity for the number and location of cooling centers by neighborhood. In the future, our models will incorporate few built-environment parameters, such as the Built-up Index (BU), building volume, and Modified Normalized Difference Water Index (MNDWI), to compare goodness of fit with the current model version. We are also studying UHI mitigation strategies in the urban canopy-climate in combination with aspect ratio, which is also directed by the neighborhoods identified with a high ERII index. As the sensitivity of a community increases with the adverse environmental conditions, it is anticipated that an estimate of local pollution and temperature anomalies will help in guiding responses to the most intense heat waves, which are infrequent enough that historical data may be a poor guide. Since current resources related to mitigating heat waves impacts are based on historical weather data, it relies primarily on demographics with some input from relatively sparse temperature and air quality measurement field campaigns. However, both the demographics and the physical environment shift with time. The separation of temperature variations from demographic variations throughout the city will allow for more precise estimates of how the city should respond when demographics or temperature patterns shift.

**Author Contributions:** Conceptualization, Maryam Karimi, Samain Sabrin and Rouzbeh Nazari; Methodology, Maryam Karimi and Samain Sabrin; Software, Samain Sabrin; Validation, Samain Sabrin, Maryam Karimi and Rouzbeh Nazari; Formal Analysis, Samain Sabrin; Investigation, Samain Sabrin; Resources, Samain Sabrin; Data Curation, Samain Sabrin; Writing-Original Draft Preparation, Samain Sabrin; Writing-Review & Editing, Samain Sabrin, Maryam Karimi and Rouzbeh Nazari; Visualization, Samain Sabrin; Supervision, Maryam Karimi and Rouzbeh Nazari; Project Administration, Maryam Karimi and Rouzbeh Nazari; Funding Acquisition, Rouzbeh Nazari and Maryam Karimi. All authors have read and agreed to the published version of the manuscript.

**Funding:** This research received funding from UAB Faculty Development Grant Program.

**Conflicts of Interest:** The authors declare no conflict of interest.

## References

1. Kohler, M.; Tannier, C.; Blond, N.; Aguejidad, R.; Clappier, A. Impacts of several urban-sprawl countermeasures on building (space heating) energy demands and urban heat island intensities. A case study. *Urban Clim.* **2017**, *19*, 92–121. [CrossRef]
2. Karimi, M.; Nazari, R.; Dutova, D.; Khanbilvardi, R.; Ghandehari, M. A conceptual framework for environmental risk and social vulnerability assessment in complex urban settings. *Urban Clim.* **2018**, *26*, 161–173. [CrossRef]
3. Seto, K.C.; Shepherd, J.M. Global urban land-use trends and climate impacts. *Curr. Opin. Environ. Sustain.* **2009**, *1*, 89–95. [CrossRef]
4. Zhang, P.; Imhoff, M.L.; Wolfe, R.E.; Bounoua, L. Characterizing urban heat islands of global settlements using MODIS and nighttime lights products. *Can. J. Remote Sens.* **2010**, *36*, 185–196. [CrossRef]
5. Stone, B.; Vargo, J.; Habeeb, D. Managing climate change in cities: Will climate action plans work? *Landsc. Urban Plan.* **2012**, *107*, 263–271. [CrossRef]
6. Fahad, M.G.R.; Saiful Islam, A.; Nazari, R.; Alfi Hasan, M.; Tarekul Islam, G.; Bala, S.K. Regional changes of precipitation and temperature over Bangladesh using bias-corrected multi-model ensemble projections considering high-emission pathways. *Int. J. Climatol.* **2018**, *38*, 1634–1648. [CrossRef]
7. Limaye, V.S.; Vargo, J.; Harkey, M.; Holloway, T.; Patz, J.A. Climate change and heat-related excess mortality in the Eastern USA. *EcoHealth* **2018**, *15*, 485–496. [CrossRef]
8. Anderson, G.B.; Bell, M.L. Heat waves in the United States: Mortality risk during heat waves and effect modification by heat wave characteristics in 43 US communities. *Environ. Health Perspect.* **2011**, *119*, 210–218. [CrossRef]
9. Montero, J.; Mirón, I.; Criado-Álvarez, J.; Linares, C.; Díaz, J. Influence of local factors in the relationship between mortality and heat waves: Castile-La Mancha (1975–2003). *Sci. Total Environ.* **2012**, *414*, 73–80. [CrossRef]
10. World Health Organization. *Quantitative Risk Assessment of the Effects of Climate Change on Selected Causes of Death, 2030s and 2050s*; WHO: Geneva, Switzerland, 2014.
11. Jerrett, M.; Burnett, R.T.; Pope, C.A., III; Ito, K.; Thurston, G.; Krewski, D.; Shi, Y.; Calle, E.; Thun, M. Long-term ozone exposure and mortality. *N. Engl. J. Med.* **2009**, *360*, 1085–1095. [CrossRef]
12. Ghude, S.D.; Chate, D.; Jena, C.; Beig, G.; Kumar, R.; Barth, M.; Pfister, G.; Fadnavis, S.; Pithani, P. Premature mortality in India due to PM<sub>2.5</sub> and ozone exposure. *Geophys. Res. Lett.* **2016**, *43*, 4650–4658. [CrossRef]
13. Sun, J.; Fu, J.S.; Huang, K.; Gao, Y. Estimation of future PM<sub>2.5</sub>-and ozone-related mortality over the continental United States in a changing climate: An application of high-resolution dynamical downscaling technique. *J. Air Waste Manag. Assoc.* **2015**, *65*, 611–623. [CrossRef]
14. U.S. EPA. *The Benefits and Costs of the Clean Air Act: 1990 to 2010*; Office of Air and Radiation: Washington, DC, USA, 2011. Available online: <https://www.epa.gov/sites/production/files/2015-07/documents/fullrept.pdf> (accessed on 26 May 2020).
15. Stafoggia, M.; Schwartz, J.; Forastiere, F.; Perucci, C. Does temperature modify the association between air pollution and mortality? A multicity case-crossover analysis in Italy. *Am. J. Epidemiol.* **2008**, *167*, 1476–1485. [CrossRef]
16. Kim, S.E.; Lim, Y.-H.; Kim, H. Temperature modifies the association between particulate air pollution and mortality: A multi-city study in South Korea. *Sci. Total Environ.* **2015**, *524*, 376–383. [CrossRef]
17. Heaviside, C.; Macintyre, H.; Vardoulakis, S. The urban heat island: Implications for health in a changing environment. *Curr. Environ. Health Rep.* **2017**, *4*, 296–305. [CrossRef]
18. Birkmann, J.; Böhm, H.R.; Buchholz, F.; Büscher, D.; Daschkeit, A.; Ebert, S.; Fleischhauer, M.; Frommer, B.; Köhler, S.; Kufeld, W. Klimawandel und Raumentwicklung. Glossar Klimawandel und Raumentwicklung. *E-paper der ARL No. 10. Hanover*. 2013. Available online: <http://nbn-resolving.de/urn:nbn:de:0156-73571> (accessed on 28 January 2020).
19. Birkmann, J.; Bach, C.; Vollmer, M. Tools for resilience building and adaptive spatial governance. *Raumforsch. Raumordn.* **2012**, *70*, 293–308. [CrossRef]
20. Riegel, C.; Trum, A.; Maximini, C.; Vallée, D. *Klimaschutzteilkonzept “Anpassung an den Klimawandel für die Städte Solingen und Remscheid”*; ISB: Aachen, Germany, 2013; Available online: <http://www.bergisches-dreieck>.

- [de/fileadmin/user\\_upload/wirtschaftsregion/PDFs/Taetigkeitsbericht\\_2012\\_b.pdf](#) (accessed on 29 January 2020).
21. Leal Filho, W.; Icaza, L.E.; Neht, A.; Klavins, M.; Morgan, E.A. Coping with the impacts of urban heat islands. A literature based study on understanding urban heat vulnerability and the need for resilience in cities in a global climate change context. *J. Clean. Prod.* **2018**, *171*, 1140–1149. [[CrossRef](#)]
  22. Uddin, M.N.; Islam, A.S.; Bala, S.K.; Islam, G.T.; Adhikary, S.; Saha, D.; Haque, S.; Fahad, M.G.R.; Akter, R. Mapping of climate vulnerability of the coastal region of Bangladesh using principal component analysis. *Appl. Geogr.* **2019**, *102*, 47–57. [[CrossRef](#)]
  23. Harlan, S.L.; Ruddell, D.M. Climate change and health in cities: Impacts of heat and air pollution and potential co-benefits from mitigation and adaptation. *Curr. Opin. Environ. Sustain.* **2011**, *3*, 126–134. [[CrossRef](#)]
  24. Basu, R. High ambient temperature and mortality: A review of epidemiologic studies from 2001 to 2008. *Environ. Health* **2009**, *8*, 40. [[CrossRef](#)]
  25. Johnson, D.P.; Stanforth, A.; Lulla, V.; Lubber, G. Developing an applied extreme heat vulnerability index utilizing socioeconomic and environmental data. *Appl. Geogr.* **2012**, *35*, 23–31. [[CrossRef](#)]
  26. Reid, C.E.; O’neill, M.S.; Gronlund, C.J.; Brines, S.J.; Brown, D.G.; Diez-Roux, A.V.; Schwartz, J. Mapping community determinants of heat vulnerability. *Environ. Health Perspect.* **2009**, *117*, 1730–1736. [[CrossRef](#)]
  27. Rosenthal, J.K.; Kinney, P.L.; Metzger, K.B. Intra-urban vulnerability to heat-related mortality in New York City, 1997–2006. *Health Place* **2014**, *30*, 45–60. [[CrossRef](#)]
  28. Rosenthal, J.K.; Brechwald, D. Climate adaptive planning for preventing heat-related health impacts in New York City. In *Climate Change Governance*; Springer: Berlin/Heidelberg, Germany, 2013; pp. 205–225.
  29. Donaldson, G.; Keatinge, W.; Näyhä, S. Changes in summer temperature and heat-related mortality since 1971 in North Carolina, South Finland, and Southeast England. *Environ. Res.* **2003**, *91*, 1–7. [[CrossRef](#)]
  30. Wolf, T.; McGregor, G. The development of a heat wave vulnerability index for London, United Kingdom. *Weather Clim. Extrem.* **2013**, *1*, 59–68. [[CrossRef](#)]
  31. Méndez-Lázaro, P.; Muller-Karger, F.E.; Otis, D.; McCarthy, M.J.; Rodríguez, E. A heat vulnerability index to improve urban public health management in San Juan, Puerto Rico. *Int. J. Biometeorol.* **2018**, *62*, 709–722. [[CrossRef](#)]
  32. O’Lenick, C.R.; Wilhelmi, O.V.; Michael, R.; Hayden, M.H.; Baniassadi, A.; Wiedinmyer, C.; Monaghan, A.J.; Crank, P.J.; Sailor, D.J. Urban heat and air pollution: A framework for integrating population vulnerability and indoor exposure in health risk analyses. *Sci. Total Environ.* **2019**, *660*, 715–723. [[CrossRef](#)]
  33. Gray, A.R. Analyzing the Urban Heat Island Effect in the City of Westminster, Maryland, with Attention to Mitigative and Adaptive Measures. Master’s Thesis, Towson University, Towson, MD, USA, 2019. Available online: <http://hdl.handle.net/11603/14291> (accessed on 31 January 2020).
  34. Lesnikowski, A. Adaptation to Urban Heat Island Effect in Vancouver, BC: A Case Study in Analyzing Vulnerability and Adaptation Opportunities. Ph. D. Thesis, University of British Columbia, Vancouver, BC, Canada, 2014. Available online: <https://open.library.ubc.ca/collections/graduateresearch/310/items/1.0075852> (accessed on 31 January 2020).
  35. Sanchez, L.; Reames, T.G. Cooling Detroit: A socio-spatial analysis of equity in green roofs as an urban heat island mitigation strategy. *Urban For. Urban Green.* **2019**, *44*, 126331. [[CrossRef](#)]
  36. Santamouris, M. Recent progress on urban overheating and heat island research. Integrated assessment of the energy, environmental, vulnerability and health impact. *Synerg. Glob. Clim. Chang. Energy Build.* **2020**, *207*, 109482.
  37. Solecki, W.; Rosenzweig, C.; Pope, G.; Chopping, M.; Goldberg, R.; Polissar, A. Urban Heat Island and Climate Change: An Assessment of Interacting and Possible Adaptations in the Camden, New Jersey Region. *Environmental Assessment and Risk Analysis Element. Research Project Summary. State of New Jersey, Department of Environmental Protection, Division of Science, Research and Technology*, 5p. 2004. Available online: <https://www.state.nj.us/dep/dsr/research/urbanheat.pdf> (accessed on 15 September 2019).
  38. Solecki, W.D.; Rosenzweig, C.; Parshall, L.; Pope, G.; Clark, M.; Cox, J.; Wiencke, M. Mitigation of the heat island effect in urban New Jersey. *Glob. Environ. Chang. Part B Environ. Hazards* **2005**, *6*, 39–49. [[CrossRef](#)]
  39. State of New Jersey, Department of Health. Camden County. Available online: <https://www.state.nj.us/health/ceohs/environmental-occupational/hazardous-waste-sites/camden/> (accessed on 2 December 2019).
  40. City of Camden, Camden Redevelopment Agency. Available online: <http://camdenredevelopment.org/> (accessed on 30 November 2019).

41. Ridlington, E.; Leavitt, C. *Trouble in the Air*; Environment America Research & Policy Center: Denver, CO, USA, 2018; Available online: <https://environmentamerica.org/sites/environment/files/reports/Trouble%20in%20the%20Air%20v%20US.pdf> (accessed on 31 January 2020).
42. Jahan, K.; Orlins, J.; Hasse, J.; Everett, J.; Miller, D. Community outreach for watershed protection. *Proc. Water Environ. Fed.* **2004**, *2004*, 1364–1377. [[CrossRef](#)]
43. Lai, L.-W.; Cheng, W.-L. Air quality influenced by urban heat island coupled with synoptic weather patterns. *Sci. Total Environ.* **2009**, *407*, 2724–2733. [[CrossRef](#)]
44. Lai, L.-W.; Cheng, W.-L. Urban Heat Island and Air Pollution—An Emerging Role for Hospital Respiratory Admissions in an Urban Area. *J. Environ. Health* **2010**, *72*, 32–36.
45. Kovats, R.S.; Hajat, S. Heat stress and public health: A critical review. *Annu. Rev. Public Health* **2008**, *29*, 41–55. [[CrossRef](#)]
46. Chen, K.; Wolf, K.; Breitner, S.; Gasparrini, A.; Stafoggia, M.; Samoli, E.; Andersen, Z.J.; Bero-Bedada, G.; Bellander, T.; Hennig, F. Two-way effect modifications of air pollution and air temperature on total natural and cardiovascular mortality in eight European urban areas. *Environ. Int.* **2018**, *116*, 186–196. [[CrossRef](#)]
47. De Sario, M.; Katsouyanni, K.; Michelozzi, P. Climate change, extreme weather events, air pollution and respiratory health in Europe. *Eur. Respir. J.* **2013**, *42*, 826–843. [[CrossRef](#)]
48. Karimi, M.; Nazari, R.; Vant-Hull, B.; Khanbilvardi, R. Urban Heat Island Assessment with Temperature Maps Using High Resolution Datasets Measured at Street Level. *Int. J. Constr. Environ.* **2015**, *6*, 17–28. [[CrossRef](#)]
49. Shen, X.; Cao, L.; Liu, K.; She, G.; Ruan, H. Aboveground biomass estimation in a subtropical forest using airborne hyperspectral data. In Proceedings of the 2016 4th International Workshop on Earth Observation and Remote Sensing Applications (EORSA), Guangzhou, China, 4–6 July 2016; IEEE: Piscataway, NJ, USA, 2016; pp. 391–394.
50. Hofierka, J.; Gally, M.; Onáčillová, K.; Hofierka, J., Jr. Physically-based land surface temperature modeling in urban areas using a 3-D city model and multispectral satellite data. *Urban Clim.* **2020**, *31*, 100566. [[CrossRef](#)]
51. Equere, V.; Mirzaei, P.A.; Riffat, S. Definition of a new morphological parameter to improve prediction of urban heat island. *Sustain. Cities Soc.* **2020**, *56*, 102021. [[CrossRef](#)]
52. Dian, C.; Pongrácz, R.; Dezső, Z.; Bartholy, J. Annual and monthly analysis of surface urban heat island intensity with respect to the local climate zones in Budapest. *Urban Clim.* **2020**, *31*, 100573. [[CrossRef](#)]
53. Galdies, C.; Lau, H.S. Urban Heat Island Effect, Extreme Temperatures and Climate Change: A Case Study of Hong Kong SAR. In *Climate Change, Hazards and Adaptation Options*; Springer: Berlin/Heidelberg, Germany, 2020; pp. 369–388.
54. Chakraborty, T.; Hsu, A.; Manya, D.; Sheriff, G. Urban Heat Island Calculations for Decision Making in the United States: Characterization and Implications. *EarthArXiv*. 2020. Available online: <https://doi.org/10.31223/osf.io/59tf8> (accessed on 25 April 2020).
55. Portela, C.I.; Massi, K.G.; Rodrigues, T.; Alcântara, E. Impact of urban and industrial features on land surface temperature: Evidences from satellite thermal indices. *Sustain. Cities Soc.* **2020**, *56*, 102100. [[CrossRef](#)]
56. Sobrino, J.A.; Jiménez-Muñoz, J.C.; Sòria, G.; Romaguera, M.; Guanter, L.; Moreno, J.; Plaza, A.; Martínez, P. Land surface emissivity retrieval from different VNIR and TIR sensors. *IEEE Trans. Geosci. Remote Sens.* **2008**, *46*, 316–327. [[CrossRef](#)]
57. Stathopoulou, M.; Cartalis, C. Daytime urban heat islands from Landsat ETM+ and Corine land cover data: An application to major cities in Greece. *Sol. Energy* **2007**, *81*, 358–368. [[CrossRef](#)]
58. Ivajnsič, D.; Kaligarič, M.; Žiberna, I. Geographically weighted regression of the urban heat island of a small city. *Appl. Geogr.* **2014**, *53*, 341–353. [[CrossRef](#)]
59. Patro, S.; Sahu, K.K. Normalization: A preprocessing stage. *arxiv* **2015**, arXiv:1503.06462. [[CrossRef](#)]

